Electronic Supplementary Material (ESI) for Nanoscale.

Supplementary information

TiO_2-Modified MoS_2 Monolayer Films Enables Sensitive NH_3 Sensing at Room Temperature

Lun Tan,[1,2#], Xianzhen Liu[1#], Peng Wu[2], Liwei Cao[2], Wei Li[2], Ang Li[2,], Zhao Wang[1,*], Haoshuang Gu[1,*]*

[1]Hubei Engineering Research Center for Safety Detection and Control of Hydrogen Energy - Hubei Key Laboratory of Micro-Nanoelectronic Materials and Devices, School of Microelectronics, Hubei University, Wuhan 430062, P.R. China.

[2]Institute of Microstructure and Properties of Advanced Materials, Beijing University of Technology, Beijing, 100124, P.R. China

*Corresponding authors, E-mail: wangzhao@hubu.edu.cn; ang.li@bjut.edu.cn; guhsh@hubu.edu.cn

[#] Both authors contribute equally to this work.

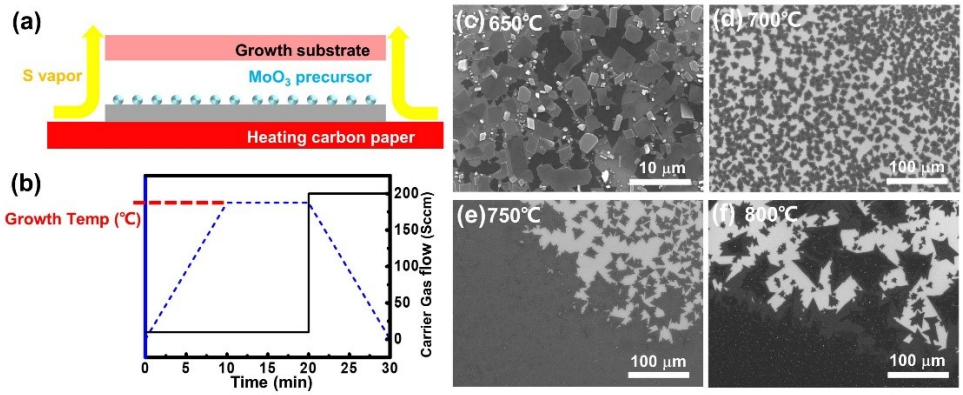

Fig.S1 The growth of monolayer MoS_2 films. (a) Schematic of the CVD apparatus. (b) Temperature profile and Ar flow during the growth process. (d-f) The SEM images of MoS2 grown at 650°C, 700°C, 750°C and 800°C, respectively. The morphology of MoS_2 at different growth temperature in 10 min is shown in **Fig S1.** When the temperature is below 700°C, many separate irregular polygonal-like crystals can be seen in **Fig S1(c)**. The Raman spectrum of those small crystals is corresponding to the MoO_2 and $MoOS_2$ which are the intermediate product during the growth of MoS_2 because of incomplete sulfurization at low temperature as shown in Fig S2. When the temperature reaches to 700°C, there are many separate MoS_2 crystals on substrate. The Raman spectrum of those small crystals in **Fig S2(a)** shows the E_{2g} and A_{1g} peaks of MoS_2, the frequency difference (Δk) between the E^1_{2g} and A_{1g} peaks is ~ 20 cm^{-1}, which is corresponding to the monolayer MoS_2. The MoS_2 crystals gradually connects into continuous polycrystalline films, when temperature rises to 750°C due to the accelerated reaction rate at high

temperature. At 800°C, Δk of films is ~ 24 cm^{-1} in Fig S2, which indicated that the films are multilayer MoS_2 films. The rapid evaporation of MoO_3 makes the pressure of MoO_3 higher on the surface of substrates, which results in the growth of multilayer MoS_2 as reported in ref.1.[1]

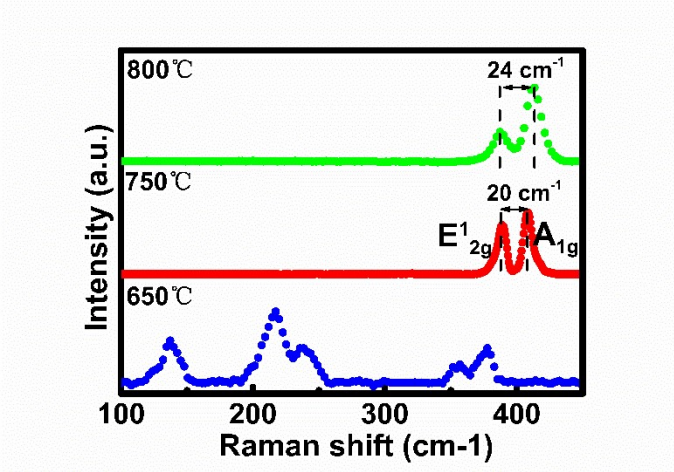

Fig.S2 The Raman spectrum of production grown at 650℃, 750℃ and 800℃, respectively.

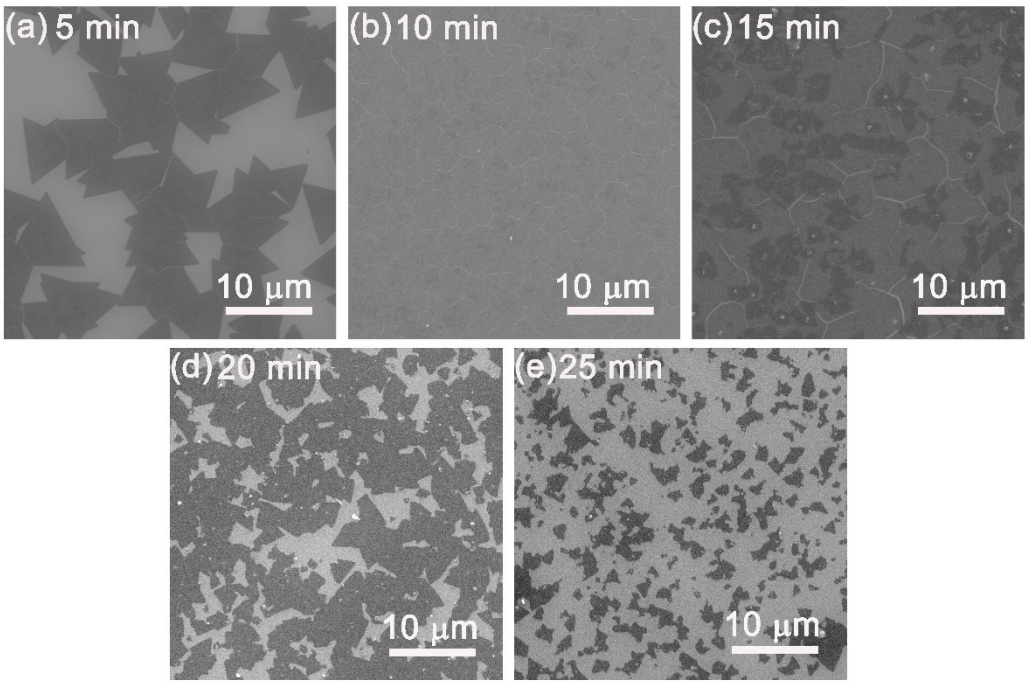

Fig.S3 SEM images of MoS_2 films at different growth time. When the growth time is shorter than 5 min, there are separated triangle-like MoS_2 nanoflakes on substrate. When the growth time is extended to 10 min, the separated MoS_2 nanoflakes connected into polycrystalline films. The new nuclei will form on the surface of MoS_2 films with the further increase of growth time, which lead to the increase of the thickness of MoS_2 films. Once the growth time exceeds 20 min, there are some pores on the MoS_2 films because of the poor thermal-stability of MoS_2 films in S insufficient environment.

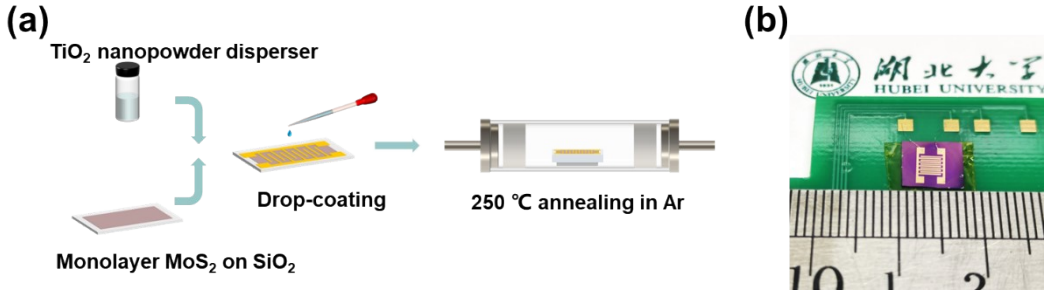

Fig. S4 Fabrication and photography of TiO_2 modifying MoS_2 monolayer films sensors. (a) the device was annealed at 250℃ in Ar for contacting tightly. (b) Photograph of a monolayer MoS_2 films with interdigitated electrodes.

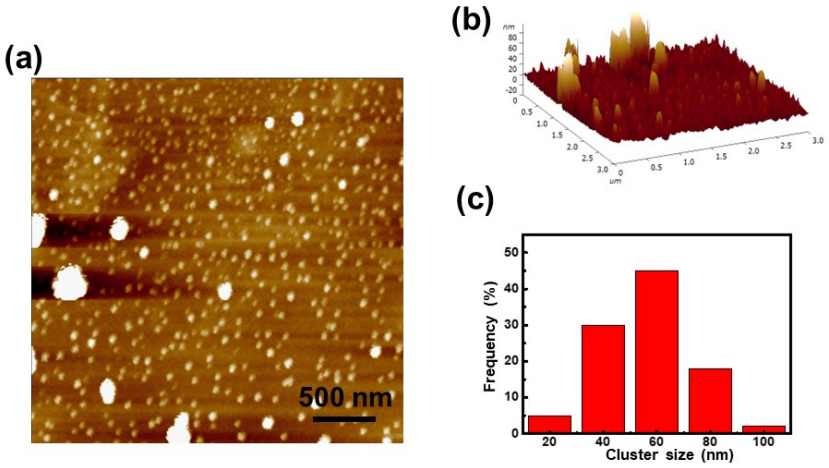

Fig. S5 AFM images of 10 nmol/cm^2 TiO_2 modifying monolayer. (a) and (b) represent the 2D and 3D AFM images of sensors. (c) particle size distribution of TiO_2 nanoparticles. The TiO_2 nanoparticles are uniformly distributed on the surface of monolayer MoS_2 films except for several big cluster (>100 nm). The average size of about those nanoparticles is about 55 nm.

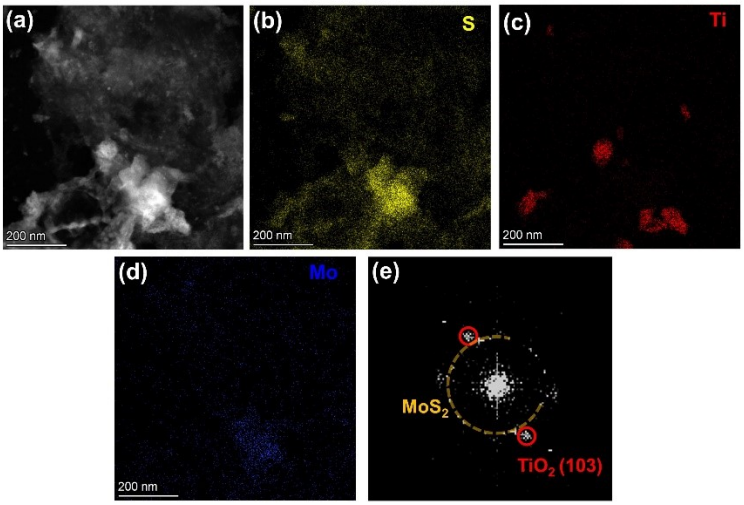

Fig. S6 HADDF images and EDS elements mappings of hybrid. It is clearly that the MoS_2 is wide distributed. the sample was obtained by scraping from the substrate, which led to the cluster and wrinkle of MoS_2 films. Therefore, there are few large area uniform flat MoS_2 films on carbon films. The size of TiO_2 nanoparticle is about 50 nm, which is consistent with the result obtained by AFM. **Fig S6 (e)** is the selected area electron diffraction (SAED) pattern of the **Fig 2(a)**.

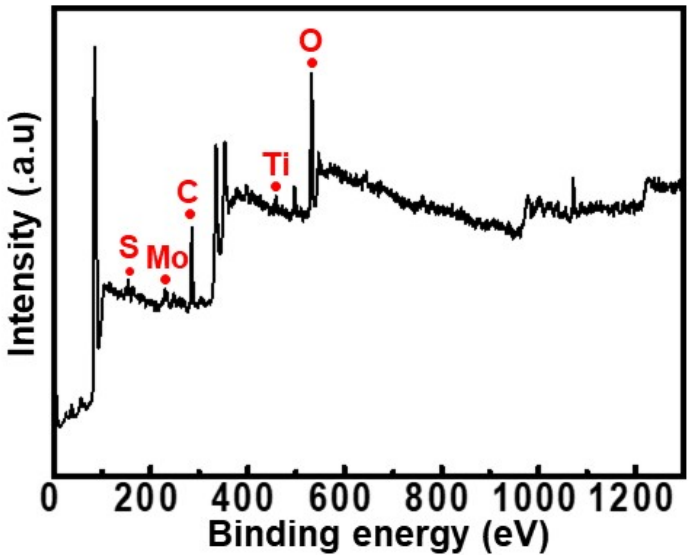

Fig. S7 The XPS spectrum of TiO_2 nanoparticles modifying monolayered MoS_2 films.

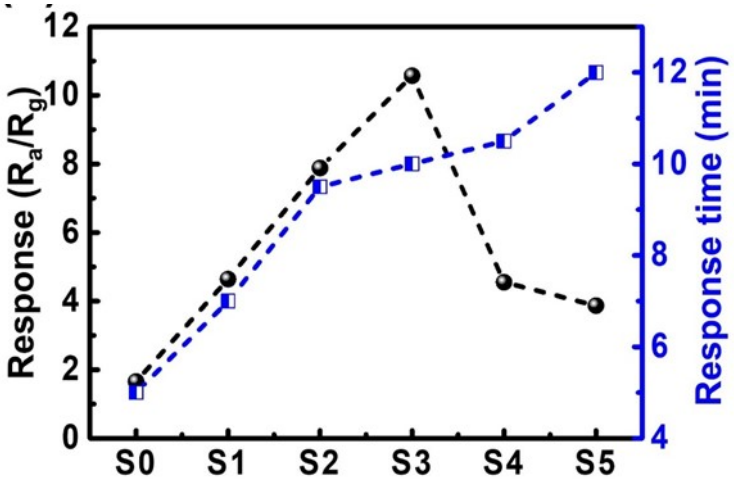

Fig. S8 Comparison of sensor response and response time of different sensors towards 500 ppm of ammonia in air. The response time varied from 5 min to 12 min with the increase amount of TiO_2 nanoparticles. -

Table. S1 Linear fit of each sensor towards 50-1000 ppm. the R^2 is greater than 0.94, indicating that the response of each sensor has a good linear relationship with the concentration of NH_3 from 50-1000 ppm.

Sample	R^2	slope
S0	0.94	0.0020
S1	0.95	0.0101
S2	0.96	0.0111
S3	0.98	0.0150
S4	0.96	0.0082

S5	0.98	0.0050

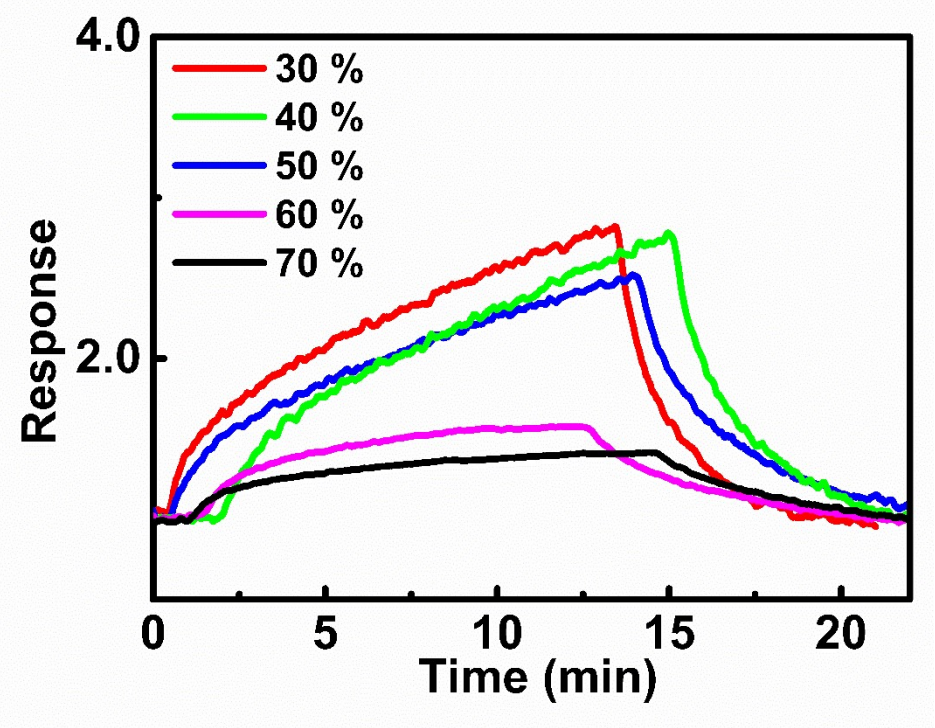

Fig. S9 The dynamic response of 30 nmol/cm^2 TiO_2 nanoparticles modifying monolayer MoS_2 films towards 50 ppm NH_3 at different humidity.

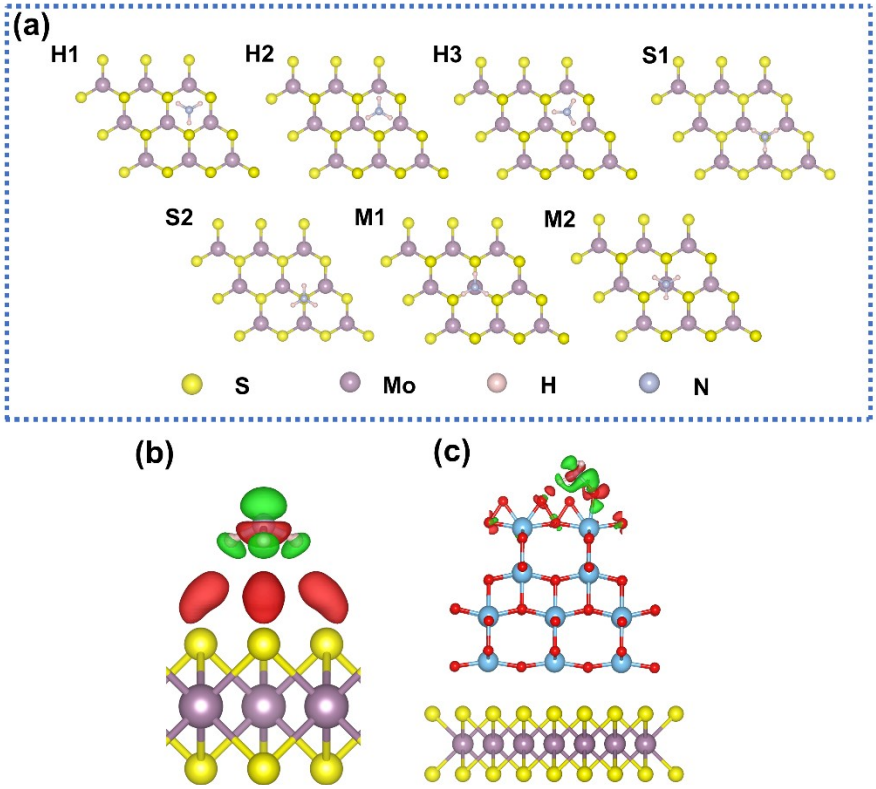

Fig. S10 DFT calculation details. (a)Top view of a monolayer MoS_2 showing hole top, S top and Mo top for N(NH_3) adsorption. (b) and (c) are isosurface plot of the electron charge density difference for NH_3 on monolayer MoS_2 and TiO_2-MoS_2 respectively. To study the adsorption of NH_3 on the MoS_2, 3 × 3 × 1 supercell of 2H-MoS_2 was built as shown in **Fig S10(a)**. A large vacuum layer of 15 Å was used to avoid interlayer interactions. A plane wave cutoff of 450 eV was consistently used during the whole process. In the process of geometry optimization, the convergency of energy and atomic force were 10^{-5} eV and 0.03 eV/Å, respectively. A Monkhorst-Park mesh of 3 × 3 × 1 for the Brillouin zone integration was employed. The adsorption energy of NH_3 molecules on MoS_2 was calculated using $E_{ads} = E_{total} - (E_{MoS2\ or\ TiO2\text{-}MoS2} + E_{NH3})$, where

E_{total} is the total energy of the NH_3 molecules on MoS_2 (or TiO_2-MoS_2) surface system, E_{MoS2} ($E_{TiO2\text{-}MoS2}$) is the energy of monolayered MoS_2 (TiO_2-MoS_2), E_{NH3} is the energy of isolated NH_3 molecule.

To explore the underlying mechanism of the significant resistance changes upon the adsorption of NH_3 molecules on MoS_2, DFT calculation was carried to analysis the NH_3 adsorption on MoS_2 as shown in **Fig. S10**. There are seven absorption sites are listed in **Fig S10(a)** which are depended on the sites of N and orientation of N-H bond. Table S2 shows the absorption energy of NH_3 molecules on each site. It is clearly that the absorption energy of H atoms near S (M1 and H1) are lower than far one (S1 and S2), which indicate that the absorption site of H in NH_3 molecule atom close S atom is more stable. this is consistent with the charge density difference of absorption system in **Fig. S10(b)** because the obvious charge transfer between H and S atoms. The blue area and red area represent electrons depletion and accumulation, respectively. It is clearly shown that the electrons were transferred from NH_3 to MoS_2, which resulted in the decrease of the resistance when MoS_2 exposed to NH_3 and this is consistent with the experimental results of bare MoS_2 films towards NH_3. Obviously, the N atom on the Mo top and the H atom orienting to S atom has small absorption energy, which is consistent with the result of the easily charge transferring between S and H atoms in **Fig S10 (a)**. Isosurface plot of the electron charge density difference for NH_3 on TiO_2-MoS_2 is shown in the

Fig. S10(c). It shows that the NH_3 molecule interact with O atoms of TiO_2, which may cause the decrease of sensor resistance. The table S2 shows the absorption energy of NH_3 molecule absorbed on the surface of MoS_2 and TiO_2-MoS_2, respectively. The adsorption energy is smaller when ammonia molecule adsorbed on the TiO_2-MoS_2 surface, indicating that ammonia molecule is more easily adsorbed on the TiO_2 surface than on MoS_2 surface since TiO_2 has more active sites.

Table. S2 The adsorption energy of NH_3 molecule on different site of MoS_2 and TiO_2-MoS_2.

Absorption sites	H1	H2	H3	S1	S2	M1	M2	TiO_2-MoS_2
E_{abs} (eV)	-0.170	-0.166	-0.167	-0.110	-0.107	-0.172	-0.166	-0.69

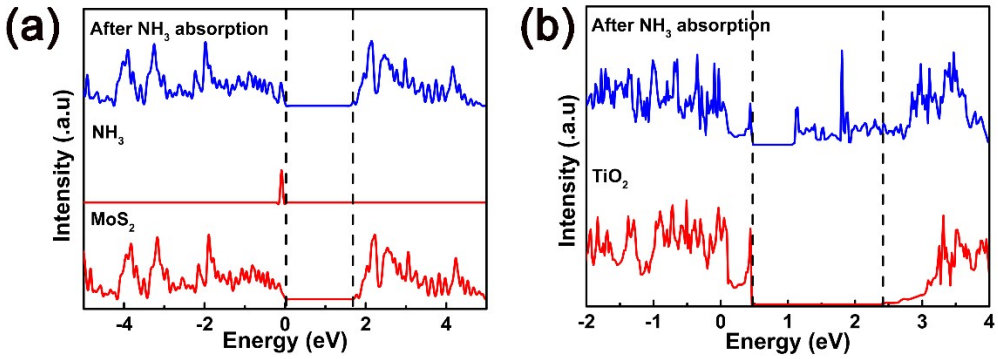

Fig. S11. The LDOS (local density of states) of before and after NH_3 absorption on MoS_2 (a) and TiO_2 (b). The absorption of NH_3 molecules result in several distinct states at the valence bands, which is close to that of pristine MoS_2 without NH_3 absorption. Therefore, the NH_3 absorption don't have a substantial effect on the electronic structures of MoS_2. Before the adsorption of the NH_3 molecules, the band gap of the TiO_2 is ~ 2 eV according to the calculation results, as shown in the **Fig S11**. After the NH_3 absorption, new electron states can be found in the band gap of TiO_2 according to the calculation results, which can be attributed to that NH_3 molecule interact with O atoms and finally lead to the narrowing of band gap to 0.7 eV. According to the first principle calculation results, the surface adsorption of NH_3 on TiO_2 will have a strong impact on the electron structure of the TiO_2, which may lead to the variation of the electrical transportation behavior of the TiO_2 host materials.

Reference

[1] J. Wei, J.-K. Huang, J. Du. Effect of the geometry of precursor crucibles on the growth of MoS2 flakes by chemical vapor deposition. *New Journal of Chemistry*. 2020, **44**, 21076-21084.